

Celogentin K, a new cyclic peptide from the seeds of *Celosia argentea* and X-ray structure of moroidin

Hayato Suzuki,^a Hiroshi Morita,^a Motoo Shiro^b and Jun'ichi Kobayashi^{a,*}

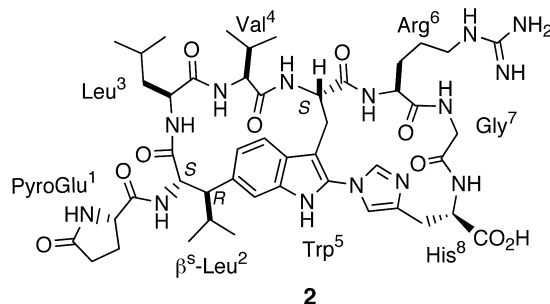
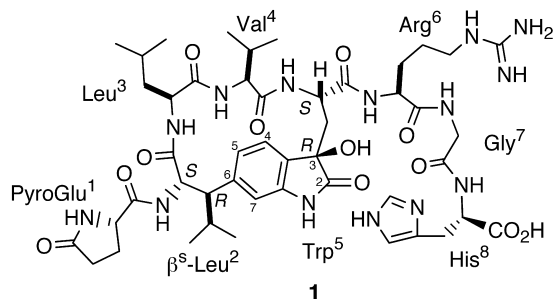
^aGraduate School of Pharmaceutical Sciences, Hokkaido University, Sapporo 060-0812, Japan

^bX-ray Research Laboratory, Rigaku Corporation, Akishima, Tokyo 196-8666, Japan

Received 24 December 2003; revised 15 January 2004; accepted 19 January 2004

Abstract—A new cyclic peptide with a 3-hydroxyoxindole ring, celogentin K (**1**), has been isolated from the seeds of *Celosia argentea* and the structure including its absolute stereochemistry was assigned by using extensive NMR, MS/MS, and CD spectra. The stereostructure of a known related bicyclic peptide, moroidin (**2**), was confirmed by a single crystal X-ray diffraction analysis.
© 2004 Elsevier Ltd. All rights reserved.

A series of celogentins A–H and J^{1,2} as well as moroidin (**2**)^{3,4} isolated from the seeds of *Celosia argentea* (Amaranthaceae) are unique cyclic peptides containing a bicyclic ring system, an unusual C–N bond formed by Trp and His residues, and an unusual amino acid, β -substituted Leu (β^s -Leu). Among them, celogentin C showed a potent inhibition of tubulin polymerization comparable to that of vinbrastine.¹ These unusual ring systems have attracted great interest as targets for biosynthetic and synthetic studies.⁵ During our continuous search for structurally unique and biogenetically interesting peptides from *C. argentea*, we isolated a new cyclic peptide with a 3-hydroxyoxindole ring, celogentin K (**1**). In addition, the stereostructure of a known related bicyclic peptide, moroidin (**2**), was established by a single crystal X-ray diffraction analysis. Here we describe the isolation and structure elucidation of celogentin K (**1**) and the X-ray structure of moroidin (**2**).



1. Isolation of celogentin K

The seeds of *C. argentea* were extracted with MeOH, and the MeOH extract was in turn partitioned with hexane, EtOAc, and *n*-BuOH. *n*-BuOH-soluble materials were subjected to a Diaion HP-20 column (MeOH/H₂O, 0:1→1:0), in which a fraction eluted with 60% MeOH was purified by an amino silica gel column (CHCl₃/MeOH/H₂O, 7:3:0.5→6:4:1) followed by C₁₈ HPLC (17% CH₃CN/0.1% CF₃CO₂H) to afford celogentin K (**1**, 0.00002% yield) as colorless solids together with moroidin (**2**)⁴ and celogentins A–H and J.^{1,2}

2. Structure elucidation of celogentin K (**1**)

FABMS data of celogentin K (**1**) {[α]_D²⁴ = -51° (c 0.5, 50%

MeOH)} showed the pseudomolecular ion at *m/z* 1021 (M+H)⁺, and the molecular formula, C₅₀H₆₉N₁₄O₁₀, was established by HRFABMS [*m/z* 1021.5221, (M+H)⁺, Δ +0.2 mmu]. IR absorptions implied the presence of hydroxyl (3400 cm⁻¹) and amide carbonyl groups

Keywords: Cyclic peptide; Celogentin K; Moroidin; NMR; MS/MS; CD; X-ray.

* Corresponding author. Tel.: +81-11-706-4985; fax: +81-11-706-4989; e-mail address: jkobay@pharm.hokudai.ac.jp

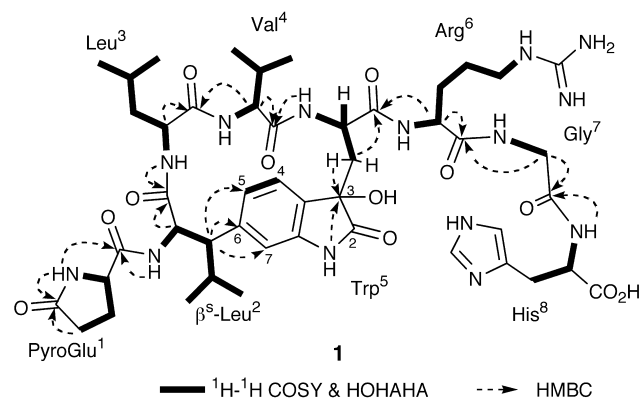


Figure 1. Selected 2D NMR correlations for celogentin K (**1**).

(1660 cm^{-1}). Standard amino acid analysis of the hydrolysates of **1** showed the presence of each 1 mol of glutamic acid (Glu), leucine (Leu), valine (Val), arginine (Arg), glycine (Gly), and histidine (His). The ^1H NMR (Table 1) spectrum of **1** in $\text{DMSO-}d_6$ at 310 K showed eight proton resonances (δ 3.74–5.05), which were indicative of α -protons of amino acid residues. The presence of six methyl groups, nine methylenes, 16 methines, one sp^3 quaternary carbon, and six olefins was indicated by the ^{13}C NMR (Table 1) spectrum. Among them, one quaternary carbon (δ_{C} 73.50) was ascribed to that bearing an oxygen. The unusual amino acids, β -substituted Leu (β^{s} -Leu) and 2,6-substituted Trp (Trp), were revealed by analysis of the ^1H and ^{13}C NMR data (Table 1) using ^1H - ^1H COSY, HOHAHA, HMQC, and HMBC experiments. The carbonyl signal (δ 179.34) was assigned as C-2 in an oxindole ring of Trp⁵. The presence of the oxindole ring with a hydroxyl at C-3 of Trp⁵ was implied by HMBC cross-peaks for H- β 1 and NH to C-3 (Fig. 1). The UV absorption (ϵ 1760) at 268 nm different from that (283 nm, ϵ 4600) of moroidin (**2**) with an indole ring supported the presence of an oxindole ring. These data combined with observation of ten carbonyl signals (δ 168.55–179.34) including a PyroGlu residue in the ^{13}C NMR spectrum suggested that **1** was an octapeptide.

The cyclic peptide nature, which was different from the bicyclic ring system of moroidin (**2**), and the sequence (PyroGlu¹- β^{s} -Leu²-Leu³-Val⁴-Trp⁵-Arg⁶-Gly⁷-His⁸) of celogentin K (**1**) were elucidated by detailed analysis of HMBC correlations as shown in Figure 1. The connection between C β of β^{s} -Leu² and C-6 of Trp⁵ was deduced from HMBC correlations for H- β of β^{s} -Leu² to C-5, 6, and 7 of Trp⁵. The HMBC correlations of H α and NH to carbonyl carbon in each residue revealed the whole sequence of celogentin K to be **1** (Fig. 1).

Further evidence supporting the proposed structure of **1** was provided by tandem mass spectrometry through examination of the collision-induced dissociation (CID) mass spectrum of the $(\text{M}+\text{H})^+$ ions.⁶ Negative ion FABMS/MS spectra of **1** showed characteristic patterns for charge-remote fragmentation, probably due to the presence of the carboxylate group of His.⁷ Product ion peaks generated by fissions of amide bonds were prominently observed (Fig. 2).

The relative stereochemistry around β^{s} -Leu² and Trp⁵ in **1**

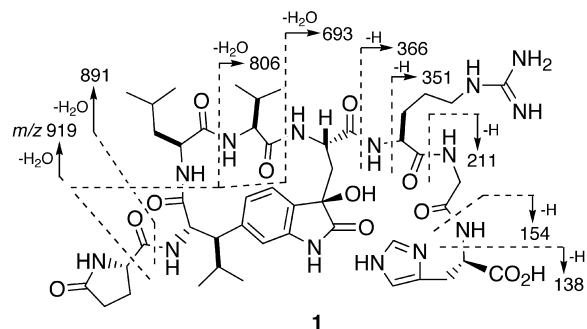


Figure 2. Fragmentation patterns observed in negative ion FABMS/MS spectrum of celogentin K (**1**) (precursor ion; m/z 1019.5).

were deduced from NOESY correlations and $^3J_{\text{H-H}}$ coupling constants as shown in computer-generated 3D drawing (Fig. 3). The absolute configurations of the PyroGlu¹, Leu³, Val⁴, Arg⁶, and His⁷ residues in celogentin K (**1**) were assigned as all L-configurations by chiral HPLC analysis of the hydrolysates of **1**. The absolute configurations of C α and C β of the β^{s} -Leu² and C α of the Trp⁵ residue were assigned from NOESY correlations (Fig. 4), which showed relation with L-Leu³ and L-Val⁴. The ring conformation deduced from such NOESY relations was consistent with those of moroidin³ and celogentins A–H and J.^{1,2} The absolute stereochemistry of C-3 of Trp⁵ was elucidated to be *R* by the CD spectrum showing positive curves at 264 ($[\theta]+10000$) and 294 nm ($[\theta]+2200$) and a negative one at 238 nm ($[\theta]-33000$) (Fig. 5).⁸ Therefore, the stereostructure of celogentin K was concluded to be **1**.

Biogenetically, celogentin K (**1**) might be derived from moroidin (**2**), by oxidation of Trp⁵ followed by C–N bond cleavage between C-2 of Trp⁵ and imidazol ring of His⁸.

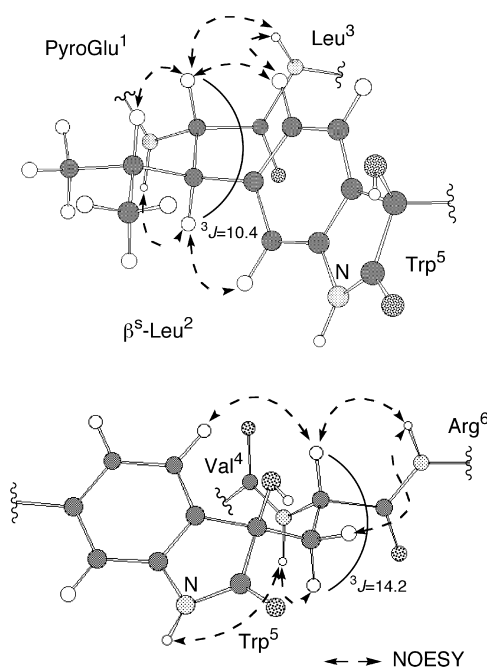


Figure 3. Selected NOESY correlations, $^3J_{\text{H-H}}$ couplings and relative stereochemistry for two units around Trp⁵ in celogentin K (**1**).

Table 1. ^1H and ^{13}C NMR data of celogentin K (**1**) in $\text{DMSO}-d_6$ at 310 K

	δ_{H} [int. mult, J (Hz)]		δ_{C}	NOE relationship
PyroGlu¹				
α	4.08 (1H, m)	α	55.07	PyroGlu ¹ : H γ ; β^{s} -Leu ² : H α , β , NH
β	1.69 and 2.25 (2H, m)	β	25.40	PyroGlu ¹ : NH; β^{s} -Leu ² : H α , β , NH
γ	2.09 (2H, t, 8.3)	γ	28.99	PyroGlu ¹ : NH;
NH	7.87 (1H, s)	δ	177.41	β^{s} -Leu ² : H α , β , NH
		C=O	172.28	
β^{s}-Leu²				
α	4.86 (1H, t, 10.4)	α	53.36	β^{s} -Leu ² : H γ , δ ; Leu ³ : H α , β , NH; Val ⁴ : H α ; Trp ⁵ : H α , H4, 5, 7
β	2.97 (1H, m)	β	50.16	β^{s} -Leu ² : H δ , NH; Trp ⁵ : H4, 5, 7, NH1
γ	2.05 (1H, m)	γ	26.26	β^{s} -Leu ² : NH; Leu ³ : NH; Trp ⁵ : H4, 5, 7, NH1
δ	0.63 (3H, d, 6.2)	δ	16.31	Leu ³ : NH; Trp ⁵ : α , H4, 5, 7, NH1
	0.73 (3H, m)		21.51	
NH	8.62 (1H, d, 9.0)	C=O	169.35	Trp ⁵ : NH1
Leu³				
α	4.12 (1H, m)	α	51.88	Leu ³ : H γ , δ ; Val ⁴ : H α , NH
β	1.32 and 1.47 (1H, m)	β	42.13	Leu ³ : NH; Val ⁴ : H α , β , NH
γ	1.45 (1H, m)	γ	24.72	
δ	0.71 (3H, m)	δ	20.69	
	0.80 (3H, m)		23.15	
NH	8.30 (1H, d, 10.3)	C=O	172.28	Val ⁴ : H α , β , NH; Trp ⁵ : H4, 5, 7
Val⁴				
α	4.10 (1H, dd, 4.7, 8.6)	α	57.70	Val ⁴ : H γ ; Trp ⁵ : NH, H α , β , H4, 5
β	1.96 (1H, m)	β	30.54	Val ⁴ : NH; Arg ⁶ : NH
γ	0.78 (6H, m)	γ	18.10	Val ⁴ : NH; Trp ⁵ : H5
			19.36	
NH	7.30 (1H, m)	C=O	169.21	Trp ⁵ : NH, H5
Trp⁵				
α	5.05 (1H, brt, 8.0)	α	47.18	Trp ⁵ : H4, 5; Arg ⁶ : H α , β , γ , NH; Gly ⁷ : NH
β	1.47 (1H, m)	β	40.10	Trp ⁵ : H4, 5, NH, NH1; Arg ⁶ : H α , NH; Gly ⁷ : NH
	2.32 (1H, brd, 14.2)	C2	179.34	
NH1	10.28 (1H, s)	C3	73.50	Trp ⁵ : H7
H4	6.81 (1H, d, 8.0)	C4	123.55	Trp ⁵ : H7; Arg ⁶ : NH
H5	7.35 (1H, d, 8.0)	C5	120.60	Trp ⁵ : H7; Arg ⁶ : NH
H7	6.42 (1H, s)	C6	138.10	
NH	8.24 (1H, m)	C7	112.68	
		C8	140.30	
		C9	128.43	
		C=O	172.13	
Arg⁶				
α	4.32 (1H, q, 7.0)	α	52.18	Arg ⁶ : H γ , NH ϵ ; Gly ⁷ : H α , NH; His ⁸ : NH, H2
β	1.54 (1H, m)	β	29.73	Arg ⁶ : NH; Gly ⁷ : H α , NH
	1.69 (1H, m)	γ	23.89	
γ	1.48 (2H, m)	δ	40.34	
δ	3.10 (2H, m)	ϵ	156.89	
ϵ (NH)	7.81 (1H, br t, 5.4)	C=O	171.77	
NH	7.50 (1H, m)			
Gly⁷				
α	3.74 (2H, m)	α	41.68	His ⁸ : H α , β , NH, H2
NH	8.46 (1H, t, 6.4)	C=O	168.55	His ⁸ : H α , β , NH
His⁸				
α	4.50 (1H, q, 7.5)	α	51.58	His ⁸ : H2:
β	2.99 (1H, m)	β	27.04	His ⁸ : H2, NH
	3.11 (1H, m)	C1	130.34	
H2	7.22 (1H, m)	C2	116.87	
H4	8.60 (1H, m)	C4	133.93	His ⁸ : NH:
NH	8.24 (1H, m)	C=O	171.41	

Celogentin K (**1**) exhibited a weak inhibitory effect on polymerization of tubulin (20% inhibition at 100 μM) as compared to that of moroidin (**2**, IC_{50} 3.0 μM).

3. X-ray structure of moroidin (**2**)

Moroidin (**2**) isolated from *C. argentea* was crystallized

from methanol–water as colorless needles, dec. 280 °C. The asymmetric unit contains two molecules (**A** and **B**) of **2** and 14 water molecules, giving a calculated density of 1.179 g cm^{-3} . The ORTEP drawings of conformers **A** and **B** were shown in Figures 6 and 7, respectively. The configurations at seven chiral centers in **2** obtained from X-ray analysis corresponded well to those proposed previously.^{3,4}

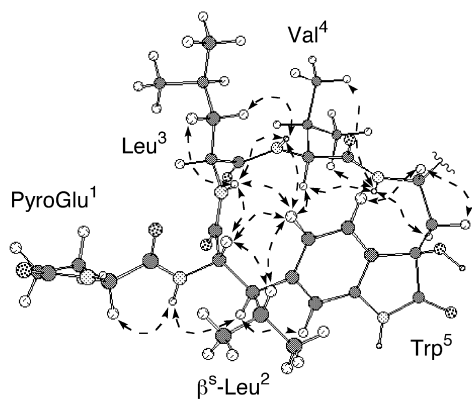


Figure 4. The ring conformation with selected NOESY correlations in celogentin K (1).

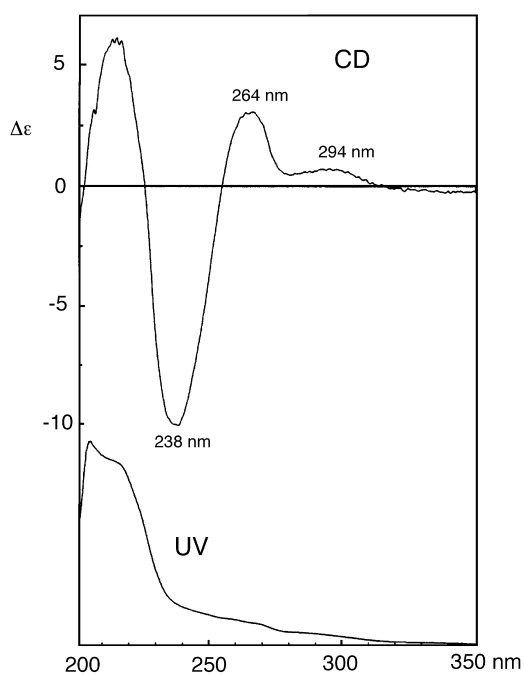


Figure 5. CD and UV spectra of celogentin K (1) in MeOH.

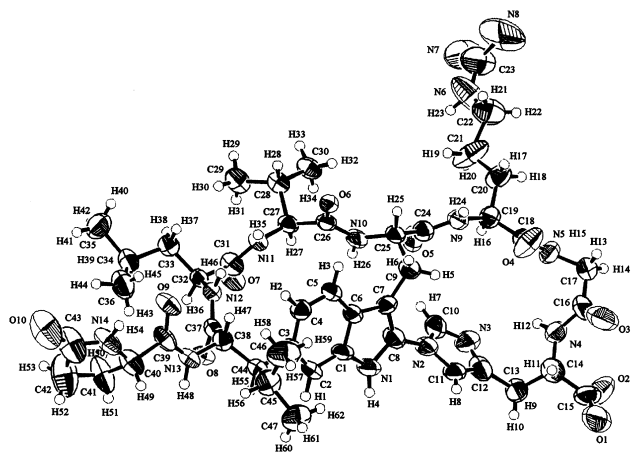


Figure 6. ORTEP drawing for conformer A of moroidin (2).

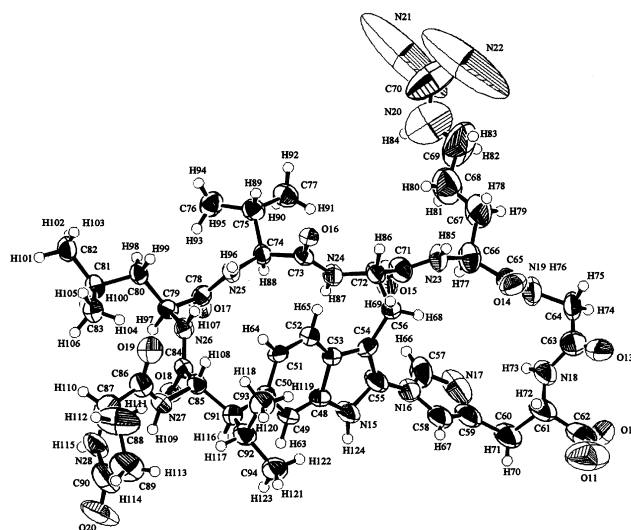


Figure 7. ORTEP drawing for conformer B of moroidin (2).

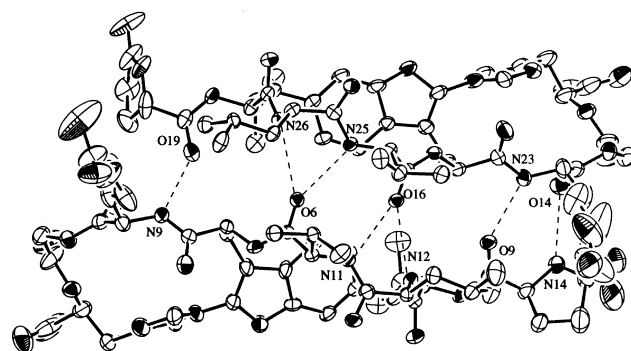


Figure 8. Two conformationally different molecules in the asymmetric unit. Broken lines show H-bonded contacts between conformers A and B for moroidin (2).

The ϕ and ψ -angles of the backbone of conformers A and B of moroidin (2) are summarized in Table 1, which shows that all (ϕ, ψ)-values lie in the β -region allowed for L-amino acids with the exception of the (ϕ, ψ)-value for Leu³ and Gly⁷. The conformation of the two respective moroidin molecule is essentially the same except for pyroGlu¹ residue. There are differences in the (ϕ, ψ)-values of pyroGlu¹ residue. The slightly twisting ω value of Arg⁶ and (ϕ, ψ)-value for Gly⁷ in the left handed α -helix region is considered to be caused by the highly constrained 14-membered ring system including the imidazol ring. Cyclic peptides are constrained as they contain turns in the backbones and these turns are often stabilized by intramolecular hydrogen bonds. There are no intramolecular hydrogen bonds in both conformers. The asymmetric unit consists of a pair of moroidin molecules, each of which forms seven hydrogen bonds linking N9, N11, N12, N14, N23, N25, and N26 of each molecule to the opposite CO moiety (see Fig. 8 and hydrogen-bond parameters listed in Table 3). Two molecules of 2 are also involved in peptide–water interactions with eight water molecules.

Table 2. Parts of torsion angles (°) along each peptide backbone of conformers **A** and **B** for moroidin (**2**)

Residue or angles	A			B		
	ϕ	ψ	ω	ϕ	ψ	ω
PyroGlu ¹	138 (2)	176 (1)	180 (1)	108 (2)	−8 (2)	−176 (1)
β^5 -Leu ²	−98 (1)	114.3 (8)	−173.8 (7)	−103 (1)	115.1 (9)	−174.5 (8)
Leu ³	−106.8 (8)	−48 (1)	−173.7 (8)	−103.7 (9)	−52 (1)	−174 (1)
Val ⁴	−142.1 (9)	126.8 (9)	172.5 (9)	−140 (1)	124.3 (9)	168 (1)
Trp ⁵	−143 (1)	166.1 (8)	174.9 (8)	−140 (1)	163 (1)	172 (1)
Arg ⁶	−128 (1)	157.0 (8)	170.1 (8)	−127 (1)	163.3 (9)	169 (1)
Gly ⁷	79 (2)	29 (3)	−179 (1)	65 (2)	32 (2)	−178 (1)
His ⁸	−69 (2)			−57 (2)		
C4–C3–C44–C38	45 (2)		C51–C50–C91–C85	42 (1)		
C3–C44–C38–C37	56 (1)		C50–C91–C85–C84	57.5 (8)		
C6–C7–C9–C25	−87 (2)		C53–C54–C56–C72	−86 (1)		
N10–C25–C9–C7	17 (1)		N24–C72–C56–C54	25 (1)		
N4–C14–C13–C12	−55 (2)		N18–C61–C60–C59	−61 (2)		
N3–C12–C13–C14	88 (2)		N17–C59–C60–C61	80 (2)		
C7–C8–N2–C10	−65 (2)		C54–C55–N16–C57	−62 (3)		

4. Experimental

4.1. General methods

¹H spectra were recorded in DMSO-*d*₆ on a 600 MHz spectrometers (Bruker AMX600) using 2.5 mm micro cells (Shigemi Co. Ltd.) at 310 K, while ¹³C NMR spectra were measured on a 150 MHz spectrometer. The NMR sample of celogentin K (**1**) was prepared by dissolving 2.0 mg in 30 μ L of DMSO-*d*₆ and chemical shifts were reported using residual DMSO-*d*₆ (δ_{H} 2.50 and δ_{C} 39.5) as internal standards. Standard pulse sequences were employed for the 2D NMR experiments. COSY, HOHAHA, and NOESY spectra were measured with spectral widths of both dimensions of 4800 Hz, and 32 scans with two dummy scans were accumulated into 1K data points for each of 256 *t*₁ increments. NOESY and HOHAHA spectra in the phase sensitive mode were measured with a mixing time of 800 and 30 ms, respectively. For HMQC spectra in the phase sensitive mode and HMBC spectra, a total of 256 increments of 1K data points were collected. For HMBC spectra with Z-axis PFG, a 50 ms delay time was used for long-range C–H coupling. Zero-filling to 1K for *F*₁ and multiplication with squared cosine-bell windows shifted in both dimensions were performed prior to 2D Fourier transformation. FABMS was measured on a JEOL JMS-HX110 by using glycerol as matrix.

4.2. Material

The seeds of *Celosia argentea* were purchased from Uchida Wakanyaku Co. in 1996. The botanical identification was made by Mr. N. Yoshida, Health Sciences University of Hokkaido. A voucher specimen has been deposited in the herbarium of Hokkaido University.

4.3. Extraction and isolation

The seeds (13.5 kg) of *C. argentea* were crashed and extracted with MeOH (18 L \times 3), and the MeOH extract was in turn partitioned with hexane, EtOAc, and *n*-BuOH. The *n*-BuOH-soluble materials were subjected to a Diaion

Table 3. Hydrogen bonds for moroidin (**2**)

A ^a	D ^a	H ^a	Distance (Å)		Angle (°), A···H–D
			A···D	A···H	
O(1)	N(28) ⁽¹⁾	115	2.83(2)	1.9	175
O(6)	N(25)	96	2.953(9)	2.1	166
O(6)	N(26)	107	2.986(9)	2.2	148
O(7)	N(15) ⁽⁴⁾	124	2.88(1)	2.0	161
O(9)	N(23)	85	2.90(1)	2.0	166
O(10)	N(5) ⁽⁵⁾	15	2.92(2)	2.3	130
O(14)	N(14)	54	2.85(1)	2.0	163
O(16)	N(11)	35	2.97(1)	2.1	161
O(16)	N(12)	46	2.967(8)	2.2	148
O(17)	N(1) ⁽⁸⁾	4	2.97(1)	2.1	174
O(19)	N(9)	24	2.86(2)	2.0	165
O(2)	N(22) ⁽²⁾	b	3.31(4)		
O(3)	N(7) ⁽³⁾	b	3.06(3)		
O(3)	N(22) ⁽²⁾	b	3.17(4)		
O(11)	N(8) ⁽⁶⁾	b	2.99(5)		
O(12)	N(8) ⁽⁶⁾	b	3.24(4)		
O(13)	N(7) ⁽⁶⁾	b	2.87(3)		
A	D (water)				
O(1)	O(32) ⁽¹⁾		3.12(9)		
O(1)	O(34) ⁽²⁾		2.82(4)		
O(2)	O(23)		2.99(3)		
O(2)	O(28)		2.71(2)		
O(2)	O(33)		2.80(6)		
O(5)	O(21) ⁽⁴⁾		2.92(2)		
O(8)	O(24)		2.68(2)		
O(11)	O(27)		2.72(3)		
O(12)	O(25)		2.79(2)		
O(15)	O(31)		3.11(4)		
O(18)	O(22)		2.77(3)		
O(18)	O(32)		3.19(9)		
O(20)	O(26) ⁽⁷⁾		2.78(3)		
O(20)	O(32)		3.48(7)		
O(20)	O(34) ⁽⁹⁾		3.20(4)		

Symmetry operators: (1) +1+X, −1+Y, +Z; (2) +1+X, +Y, −1+Z; (3) +1+X, +Y, +Z; (4) +X, −1+Y, +Z; (5) +X, +Y, +1+Z; (6) +1+X, +Y, +1+Z; (7) +X, +1+Y, +Z; (8) −1+X, +1+Y, +Z; (9) +X, +1+Y, −1+Z; (10) +X, +Y, −1+Z; (11) −1+X, +1+Y, +1+Z; (12) +1+X, −1+Y, −1+Z; (13) −1+X, +Y, +1+Z; (14) +X, −1+Y, +1+Z; (15) −1+X, +Y, +Z; (16) −1+X, +Y, −1+Z.

^a A=proton acceptor, D=proton donor, H=number of hydrogen atom.

^b Hydrogen atoms could not be detected.

HP-20 column (MeOH/H₂O, 0:1→1:0), in which a fraction eluted with 60% MeOH was purified by an amino silica gel column (CHCl₃/MeOH/H₂O, 7:3:0.5→6:4:1) followed by C₁₈ HPLC [CAPCELL PAK AQ, 5 μm, Shiseido Fine Chemicals, 10×250 mm; eluent, CH₃CN/0.1% CF₃CO₂H, (17:83); flow rate, 2 mL/min; UV detection at 210 nm] to afford celogentin K (**1**, 0.00002% yield) together with moroidin (**2**)⁴ and celogentins A–H and J.^{1,2}

4.3.1. Celogentin K (1). Colorless solid; $[\alpha]_D^{24} = -51^\circ$ (*c* 0.5, 50% MeOH); UV (MeOH) λ_{\max} (ϵ): 268 (1760) nm; IR (KBr) ν_{\max} 3400, 2960, 1660, and 1545 cm⁻¹; ¹H and ¹³C NMR (Table 1); FABMS *m/z* 1021 (M+H)⁺; HRFABMS *m/z* 1021.5221 (M+H; calcd for C₅₀H₇₀N₁₄O₁₀, 1021.5219); CD (MeOH) λ_{\max} (θ): 264 ([θ]+10000), 294 ([θ]+2200), and 238 nm ([θ]-33000).

4.4. Amino acid analysis of **1**

Solution of **1** (0.05 mg) in 6 N HCl was heated at 110 °C for 24 h in a sealed tube. After cooling, solution was concentrated to dryness. The hydrolysate was dissolved in 0.02 N HCl and subjected to amino acid analyzer.

4.5. Absolute configurations of amino acids

Solution of **1** (0.1 mg) in 6 N HCl (0.2 mL) was heated at 110 °C for 24 h. The solution was concentrated to dryness. The residue was dissolved in H₂O (50 μL) and chiral HPLC analyses were carried out using a SUMICHIRAL OA-5000 column (Sumitomo Chemical Industry; 150 mm; 25 °C, detection at 254 nm). Retention times (min) of authentic amino acids were as follows: L-Glu (19.2), D-Glu (24.2), L-Val (6.1), D-Val (9.0), L-Arg (2.2), D-Arg (2.4), L-His (9.4), D-His (7.8), L-Leu (13.6), D-Leu (20.2) [eluent: MeOH/H₂O (15:85) containing 2.0 mM CuSO₄, flow rate 1.0 mL/min]; Retention times of the hydrolysate were as follows: L-Glu (19.2), L-Val (6.1), L-Arg (2.2), L-His (9.4), and L-Leu (13.6).

4.6. Microtubule assembly assay

Microtubule assembly was monitored spectroscopically by using a spectrophotometer equipped with a thermostatically regulated liquid circulator. The temperature was held at 37 °C and changes in turbidity were monitored at 400 nm. For the drug–protein studies, 10 μM of drug dissolved in 1% DMSO concentration. The turbidity changes were monitored throughout the incubation time.

4.7. X-ray analysis of moroidin (**2**)

Moroidin (**2**) was crystallized from MeOH–H₂O to give colorless needles (dec. 280 °C). Crystal data: C₄₇H₈₀N₁₄O₁₇, crystal dimensions 0.35×0.20×0.10 mm, space group *P*1 (#1), *a*=12.040 (5), *b*=13.422 (6), *c*=22.19 (1) Å, α =77.11(4)°, β =86.81(4)°, γ =63.85(4)°, *V*=3134(2) Å³, *Z*=2, *D*_{calc}=1.179 g/cm³. A crystal was coated with liquid paraffin and mounted in a loop. All measurements were made on a Rigaku RAXIS RAPID imaging plate area detector with graphite monochromated Mo K α radiation (λ =0.71075 Å). Indexing was performed from 10° oscillations that were exposed for 1800 s. The

crystal-to-detector distance was 127.40 mm. Cell constants and an orientation matrix for data collection as shown above corresponded to a primitive triclinic cell. Based on a statistical analysis of intensity distribution, and the successful solution and refinement of the structure, the space group was determined to be *P*1 (#1). The data were collected at a temperature of -180 ± 1 °C in the range of $20.0^\circ < 2\theta < 50.7^\circ$. A total of 40 oscillation images were collected. A sweep of data was done using ω scans from 130.0 to 190.0° in 5.0° step, at $\chi=45.0^\circ$ and $\phi=0.0^\circ$. The exposure rate was 360.0 [sec./°]. A second sweep was performed using ω scans from 0.0 to 140.0° in 5.0° step, at $\chi=45.0^\circ$ and $\phi=180.0^\circ$. The exposure rate was 360.0 [sec./°]. The crystal-to-detector distance was 127.40 mm. Readout was performed in the 0.100 mm pixel mode. Of the 22704 reflections that were collected, 10479 were unique (*R*_{int}=0.041); equivalent reflections were merged. The linear absorption coefficient, μ , for Mo K α radiation is 0.9 cm⁻¹. The data were corrected for Lorentz and polarization effects.

The structure was solved by direct methods and expanded using Fourier techniques. The non-hydrogen atoms were refined anisotropically. Hydrogen atoms except for guanidino moiety of Arg⁶ and water were included but not refined. The final cycle of full-matrix least-squares refinement on *F*² was based on 10456 observed reflections and 1406 variable parameters and converged (largest parameter shift was 0.01 times its esd) with unweighted and weighted agreement factors of $R1 = \sum |F_o| - |F_c| / \sum w |F_o| = 0.122 [I > 2.00\sigma(I)]$ and $wR2 = [\sum w(F_o^2 - F_c^2)^2 / \sum w(F_o^2)^2]^{1/2} = 0.348 [I > -3.00\sigma(I)]$. The standard deviation of an observation of unit weight was 1.10. Unit weights were used. The maximum and minimum peaks on the final difference Fourier map corresponded to 0.69 and $-0.41 e^- / \text{\AA}^3$, respectively.

Neutral atom scattering factors were taken from Cromer and Waber.⁹ Anomalous dispersion effects were included in *F*_c; the values for $\Delta f'$ and $\Delta f''$ were those of Creagh and McAuley.¹⁰ The values for the mass attenuation coefficients are those of Creagh and Hubbell.¹¹ All calculations were performed using the CrystalStructure crystallographic software package¹² except for refinement, which was performed using SHELXL-97. The refined fractional atomic coordinates, bond lengths, bond angles, and thermal parameters have been deposited at the Cambridge Crystallographic Data Centre (CCDC).

Acknowledgements

The authors thank Mrs. S. Oka and Miss M. Kiuchi, Center for Instrumental Analysis, Hokkaido University, for measurements of FABMS and FABMS/MS, and Mr. N. Yoshida, Health Sciences University of Hokkaido, for botanical identification. This work was partly supported by a Grant-in-Aid for Scientific Research from the Ministry of Education, Culture, Sports, Science, and Technology of Japan, and a grant from Shorai Foundation for Science and Technology.

References and notes

1. Kobayashi, J.; Suzuki, H.; Shimbo, K.; Takeya, K.; Morita, H. *J. Org. Chem.* **2001**, *66*, 6626–6633.
2. Suzuki, H.; Morita, H.; Iwasaki, S.; Kobayashi, J. *Tetrahedron* **2003**, *59*, 5307–5315.
3. Morita, H.; Shinbo, T.; Shigemori, H.; Kobayashi, J. *Bioorg. Med. Chem. Lett.* **2000**, *10*, 469–471.
4. Leung, T.-W. C.; Williams, D. H.; Barna, J. C. J.; Foti, S. *Tetrahedron* **1986**, *42*, 3333–3348. Leung, T.-W. C.; Williams, D. H.; Barna, J. C. J.; Foti, S. *J. Org. Chem.* **1989**, *54*, 1901–1904. Kahn, S. D.; Booth, P. M.; Waltho, J. P.; Williams, D. H. *J. Org. Chem.* **2000**, *65*, 8406.
5. Comber, M. F.; Moody, C. J. *Synthesis* **1992**, 731–733.
6. Eckart, K.; Schwarz, H.; Tomer, K. B.; Gross, M. L. *J. Am. Chem. Soc.* **1985**, *107*, 6765–6769.
7. Naoki, H. In *LC/MS no Jissai*. Harada, K., Oka, H., Eds.; Kodansha: Tokyo, 1996; pp 225–252.
8. Takayama, H.; Shimizu, T.; Sada, H.; Harada, Y.; Kitajima, M.; Aimi, N. *Tetrahedron* **1999**, *55*, 6841–6846.
9. Cromer, D. T.; Waber, J. T. *International tables for X-ray crystallography*; The Kynoch Press: England, 1974; Vol. IV. Table 2.2A.
10. Creagh, D. C.; McAuley, W. J. *International tables for crystallography*; Wilson, A. J. C., Ed.; Kluwer: Boston, 1992; Vol. C, pp 219–222.
11. Creagh, D. C.; Hubbell, J. H. *International tables for crystallography*; Wilson, A. J. C., Ed.; Kluwer: Boston, 1992; Vol. C, pp 200–206.
12. Crystal Structure 3.5.2, Crystal Structure Analysis Package, Rigaku and Rigaku/MSC (2000–2003).